**Solid Freeform Fabrication 2017: Proceedings of the 28th Annual International Solid Freeform Fabrication Symposium – An Additive Manufacturing Conference**
**Reviewed Paper**

# Influence of Gage Length on Miniature Tensile Characterization of Powder Bed Fabricated 304L Stainless Steel

S. Karnati[*], J. L. Hoerchler[*], F. Liou[*], J.W. Newkirk[†]

[*]Department of Mechanical and Aerospace Engineering

[†]Department of Materials Science and Engineering

Missouri University of Science and Technology, Rolla, USA

## Abstract

Miniature tensile specimens with varying aspect ratios were fabricated from 304L stainless steel (SS) made using powder bed additive manufacturing (AM) process. The tensile characteristics measured from these specimens were analyzed to assess the impact of gage length. The study found no impact upon varying gage length on yield and ultimate strength measurements. However, a significant impact was observed on strain measurements. This data was also used to perform Weibull statistics to estimate the stochastic performance of the material. Fractography was performed to visually identify the types of flaws. A comparative study with specimens fabricated from cold rolled annealed 304 SS was also performed. The Weibull parameters were used to compare the variability within cold rolled annealed and AM 304L SS. This study indicates miniature tensile testing is a robust characterization technique for obtaining representative material properties.

## Introduction

Over the past few decades, Additive Manufacturing (AM), more commonly known as 3D printing has gathered a lot of attention from manufacturing and research communities. The layer by layer build schema of AM provides vast flexibility and the feasibility towards fabricating complex geometries from a multitude of raw material feedstocks. The capabilities offered by AM are expected to significantly alter the existing production infrastructure with respect to production, assembly, and supply chain. Currently, commercial solutions based on metal powder bed processes are available under the names, Selective Laser Melting, Laser Cusing and Direct Metal Laser Sintering (DMLS). These technologies usually employ a high-powered laser to achieve consolidation of metal powder under an inert atmosphere. They can produce parts with a relatively smooth surface finish and lower assembly requirements. In theory, depending on the size of the component and the equipment's build volume, multiple parts can be built in a single cycle of a powder bed process. Parts can be laid side by side and stacked on top of each other to attain maximum production output ("Metal Additive Manufacturing Processes" 2017; Gao et al. 2015). Owing to these reasons, coupled with infinite design flexibility and manufacturing ease, the manufacturing industry has shown significant interest towards incorporating powder bed processes into their manufacturing and production lines.

Unlike the parts made from conventional subtractive manufacturing processes like machining, the properties of AM products can be very different from the feedstock material (Song et al. 2015). This is due to the fact that the complex mechanics of a powder bed process often leads to very complicated and non-equilibrium outcomes. Evidence suggests that the properties of the fabricated material could even be anisotropic. In general, the performance of powder-bed processed materials can be sensitive to fabrication conditions and are also influenced by important process attributes such as part shape, part size, orientation in the build etc. (Shamsaei et al. 2015; Olakanmi, Cochrane, and Dalgarno 2015). Anisotropies consequent of varying the orientation have been observed by researchers for several materials. Blackwell 2005, found significant differences in tensile properties of IN718L upon varying build orientation. Yadollahi et al. 2017 also found significant differences in tensile and fatigue performances of 17-4 precipitation hardening stainless steel by varying the build orientation. Differences in microstructure and flaw orientations were theorized to cause the varied material performance. Similar effects were noticed by Rao et al. 2016 during the production of the A357 aluminum alloy. The similarities among all the above-discussed works are that the anisotropy and effects of process parameter variation occur at a finer scale during AM production. Assessing the presence and scale of such anisotropy can be infeasible using existing methods that have been standardized for mechanical testing. The sizes of standard test specimens can be too large and thereby be unable to capture and study anisotropy at the desired smaller scales (ASTM E-8, 2016). In this regard, the testing of miniaturized specimens can be an efficient and economical way to characterize such anisotropy in AM materials. The smaller size of the specimens makes specimen preparation cheaper and easy. The economy of the approach also makes it feasible to perform extensive rigorous testing and assess stochastic performance easily (Salzbrenner et al. 2017).

Miniature testing methodologies, especially mini tensile testing has been a topic of study by researchers of the nuclear industry (N. F. Panayotou, S. D. Artkin, R. J. Puigh 1986; Rosinski et al. 1993). The miniature specimens were used to study irradiated material while ensuring minimal exposure to the operator. Other studies have been performed to identify the impact of specimen design, aspect ratio, thickness to width ratio etc. on property measurements. Researchers have pursued many experimental and theoretical studies to investigate and prove the validity while simultaneously developing mathematical models of the miniature testing methods. The studies concluded that testing miniature specimens can be a valid approach for estimating a material's performance life and reliably characterize its properties (Kumar et al. 2014; Lord et al. 2010; Dieter 1986). The current study involves the development and implementation of miniature tensile testing methodologies for testing metallic dog-bone shaped specimens. The novelty of the current study includes the specimen size, preparation methodology, and the test specimen's unique fixturing technique. The comparative study between cold rolled and powder bed AM fabricated materials at a multitude of gage lengths is aimed at understanding the property measurements and their relationship to their manufacturing process. The Weibull

statistics provide insights into the variability in AM material in comparison to cold rolled annealed material.

## Experimental setup and method

To study the impact of gage length on the tensile property measurements, specimens of different gage lengths were prepared and tested. The dimensions of the mini tensile specimens are shown in Figure 1. The gage length of the specimens was varied from 3mm to 6mm in 1mm increments, while the dimensions of the remaining features were kept unchanged. The specimens for testing the powder bed process fabricated material were cut from 4 blocks of 25.4mm (1") x 25.4mm (1") x 50.8m (2") 304L stainless steel. These four blocks of steel were fabricated during a single build with parameter settings optimized for maximum density. The only difference among these blocks was their location on the build plate. A Renishaw AM250 powder bed machine was used to fabricate these blocks while a Sodick wire-EDM machine was used to machine the required specimens. The various specimen designs were cut as columns along the height of the steel blocks. These columns were then sectioned at repeating 1mm thicknesses to obtain the individual specimens. By doing so, the gage length of each specimen was perpendicular to the build direction. The specimens for testing wrought material were cut from a cold rolled and annealed 304 stainless sheet of thickness 1.168mm (0.046"). The gage length of these specimens was aligned along the rolling direction.

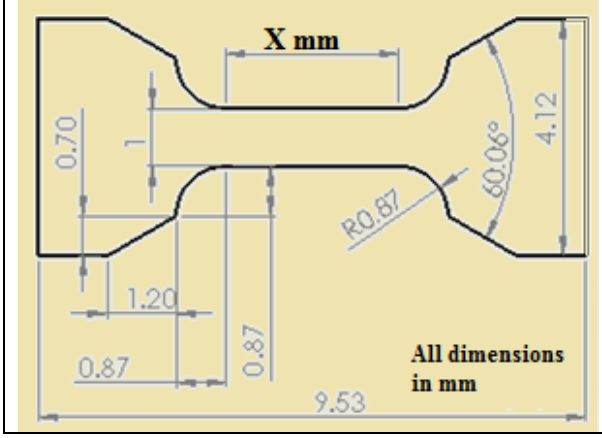


| Gage length, X (mm) |
|---|
| 3 |
| 4 |
| 5 |
| 6 |

Figure 1. Drawing of the mini tensile specimen design with the different values of gage length used for this study

Tensile testing of these specimens was performed using an Instron universal testing machine. Custom grips were manufactured and setup in order to perform the testing of mini tensile specimens. To avoid any torsion or bending during testing, the grips were designed to be self –aligning. Each self-aligning grip has two joints, which can rotate perpendicular to each other (similar to a ball and socket joint). This flexibility was expected to avoid issues of miss-alignment and ensure a uniaxial tensile testing during every test. The setup including the grips

and the extensometer is shown in Figure 2. By using the extensometer to record elongation, closed-loop, strain controlled testing was performed. An extensometer of 15.24 mm (0.6 inches) gage length was used to run these tests. Due to the small size of these specimens, setting the extensometer directly on the specimen was not feasible. The extensometer was setup on the grips of the tensile tester. It was assumed that all the deformation noted by the extensometer came from elongation of the specimen. A strain rate of 0.015mm/mm/min was used leading up to a strain of 0.01. Later, the extensometer was removed and a strain rate of 0.5mm/mm/min was then used to pull the specimen to fracture. The same strain rate schema was used for all the specimens.

A detailed statistical analysis was performed to identify the differences among the various measurements and also investigate the impact of varying the gage length. The analysis was performed using SAS and JMP software, plots of Weibull distributions were plotted using Minitab software. The estimates for the distributions were calculated using the maximum likelihood methodology. The total number of valid tests at each gage length for both the AM fabricated and cold rolled annealed materials are listed in Table 1. The fracture surfaces of the broken specimens were imaged using a scanning electron microscope to assess the fracture mechanism and identify the sources of the flaws.

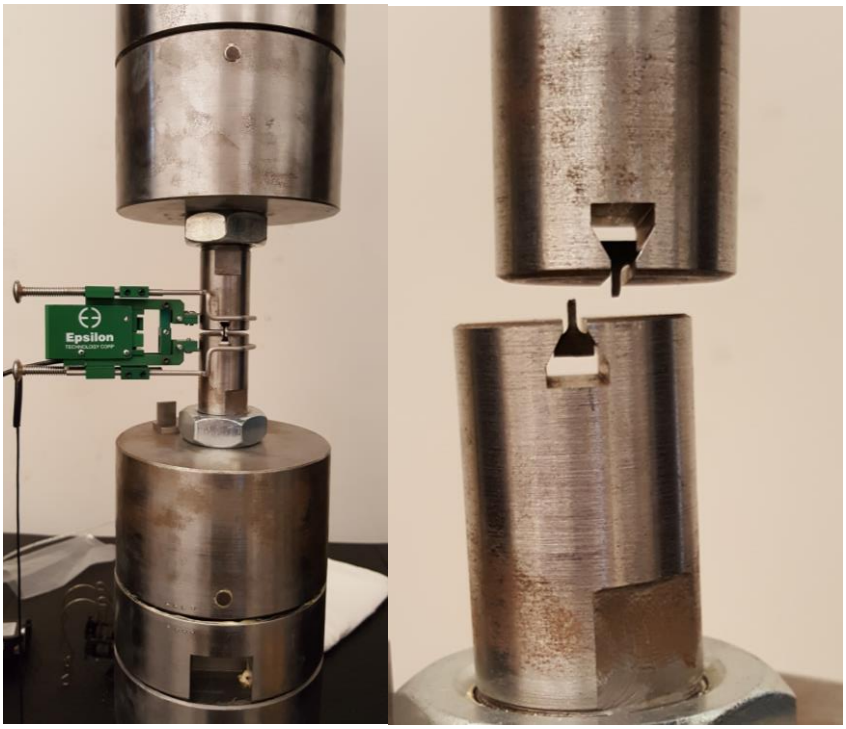


Figure 2. Self–aligning grip setup with extensometer attached on the grips (left) and broken mini-tensile specimen in the grips after completion of tensile test (right)

Table 1. Total number of specimens tested for each type of material at different gage lengths

| Gage length | Powder bed | Cold rolled annealed |
|---|---|---|
| 3 | 39 | 30 |
| 4 | 34 | 22 |
| 5 | 36 | 25 |
| 6 | 26 | 27 |

## Results and discussions

The current analysis includes a comparison of 0.2% offset Yield Strength (YS02), Ultimate Tensile Strength (UTS), and Maximum Strain (MxS). The data gathered from specimens made from cold rolled annealed material and powder bed AM material was processed by performing an analysis of variance and Weibull statistical assessment. Box plot charts of these measurements are shown in Figures 3 and 4. At each gage length, the horizontal line in the box represents the median and the box represents the range between the 25$^{th}$ and 75$^{th}$ quantile. The vertical lines represent the range between the minimum and maximum values obtained at the corresponding gage length. Finally, the asterisks represent outlier data points.

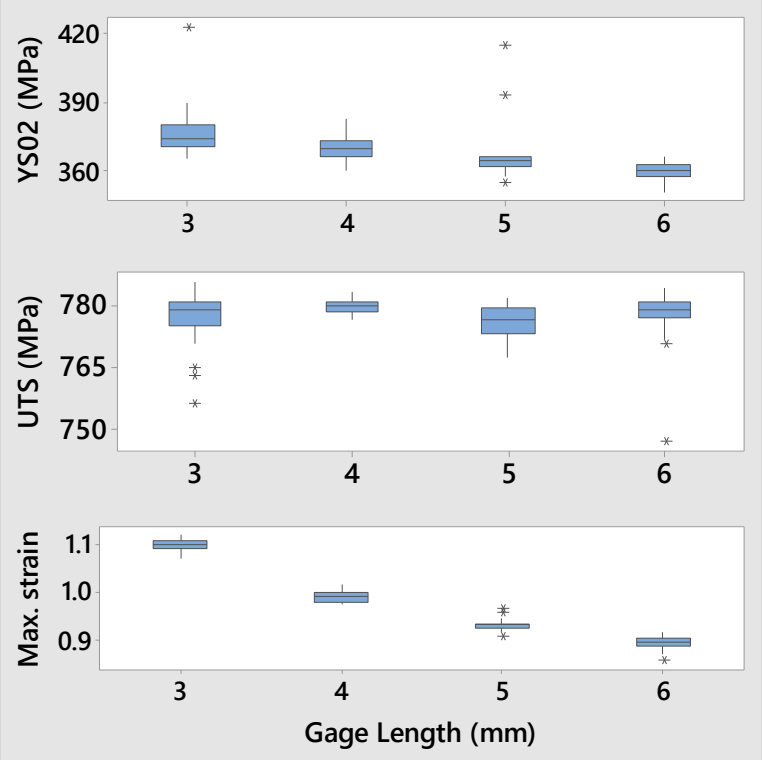


Figure 3. Box plot charts of yield strength, ultimate strength and maximum strain measurements gathered from different gage length specimens of cold rolled annealed stainless steel

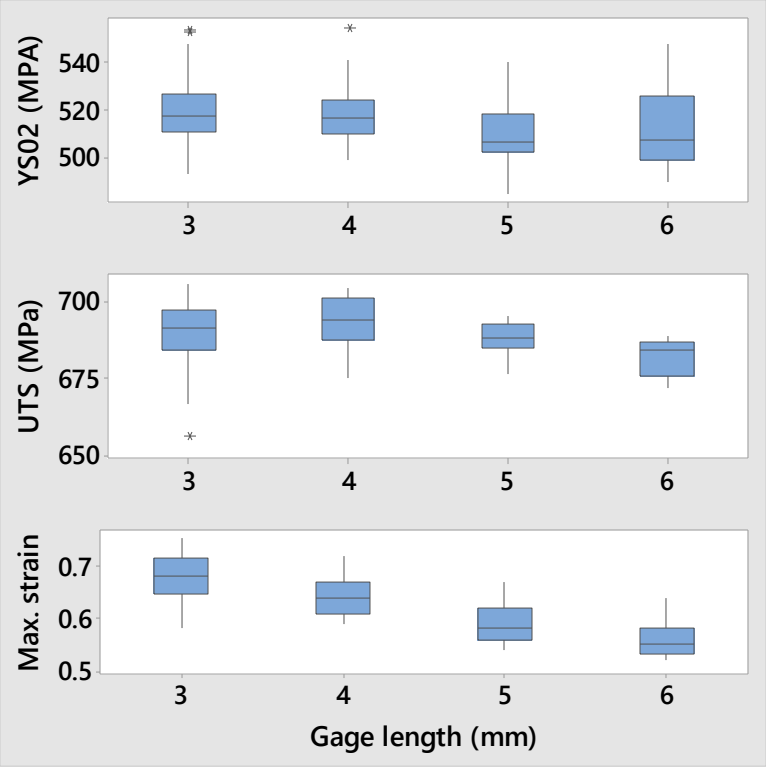


Figure 4. Box plot charts of yield strength, ultimate strength and maximum strain measurements gathered from different gage length specimens of powder bed fabricated stainless steel

Considering gage length as the only factor, a one-way factorial analysis was performed on the measurements from both cold rolled annealed and AM material. The yield strength of the AM material was observed to be higher than the cold rolled annealed material. The higher strength of the AM material can be attributed to the smaller grain size that is characteristic of the AM process. However, the ultimate tensile strength and the maximum strain values of the cold rolled annealed material were higher than the AM material. The analysis of variance revealed there were no significant differences in the yield strength and ultimate strength measurements for tests performed on the AM material. However, with varying gage lengths, a significant difference was observed among the maximum strain measurements. The same analysis on cold rolled annealed material measurements concluded there were no significant differences among the ultimate strength measurements. However, in this case, the yield strength and maximum strain measurements showed a significant difference. The statistical significance of these differences was also validated by running a Tukey's analysis of means comparison.

Unlike the AM material, the yield strength values of the cold rolled annealed material were observed to be varying with gage length. The authors theorize that this variation could be related to the larger grain size in the cold rolled annealed material. Due to the larger grain size, the authors theorize that the gage lengths investigated might not be voluminous enough to be representative of the cold rolled annealed material. With increasing gage length, the probability

of the number of larger grains within the gage length is expected to increase and thereby cause a drop in yield strength. However, the drop was not a substantial amount (10 MPa approx.) while still being statistically significant. The values of yield strength (350 MPa) and ultimate strength (690 Mpa), as noted in the certificate of test supplied with the material, were lower than the values obtained through mini tensile testing. This supports the claim that these cold rolled annealed specimens were not representative of the entire material. The higher ultimate strength could be attributed to the differences in flaw population between mini tensile specimens and standard tensile specimens. The smaller gage volume of the cold rolled annealed specimens would also have a fewer number of flaws. Therefore, these specimens could perform better during mini-tensile testing which is reflected in the larger measurements of the ultimate strength values.

The variability in property measurements of AM material was much higher than the variability in measurements from the cold rolled annealed material. The yield and ultimate tensile strength measurements on the cold rolled annealed material were very consistent and were spread over a small range (approximately 20 MPa) in comparison to AM property measurements (60-80 MPa). The wide variability in AM property measurements was suspected to be from the differences in the steel blocks used to prepare the specimens.

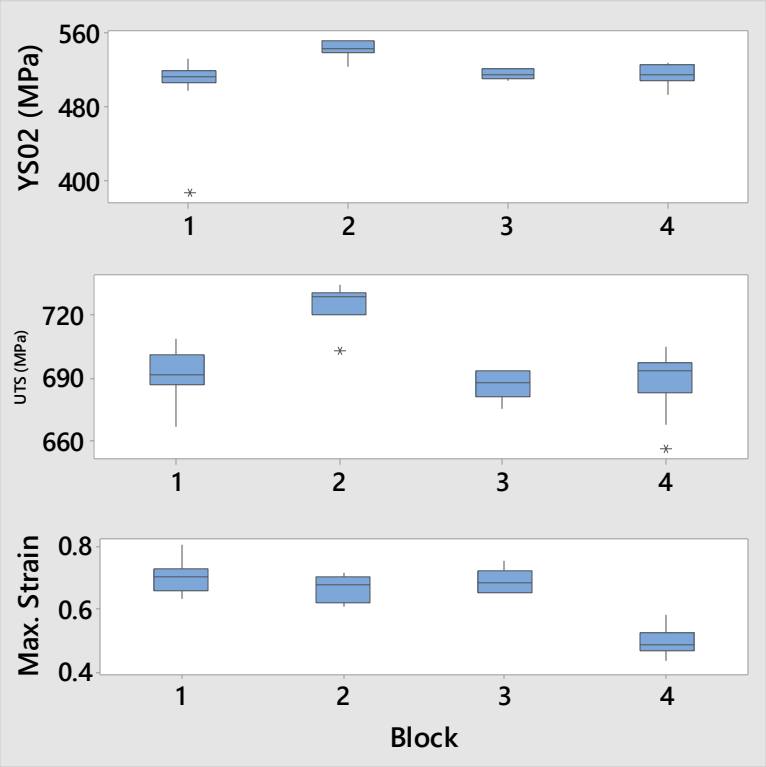


Figure 5. Yield strength (MPa), ultimate strength (MPa) and maximum strain measurements from specimens with a gage length of 3mm prepared from different blocks.

As power and other fabrication, parameters were kept the same, and all the blocks were built during a single run of the machine, the only possible source of variation was expected to be the location of these blocks on the substrate build plate. The analysis of variance was then re-investigated with gage length and the source material (as a blocking factor to isolate the variation at the source) as the factors of variation. Based on the new analysis of variance, the different source materials were confirmed to be the cause of this high variability. The yield strength, ultimate strength and maximum strain measurements of specimens with 3mm gage length gathered from the four different blocks are shown in Figure 5. The yield and ultimate strength values of specimens from block 2 were found to be higher than the specimens from the remaining blocks. The maximum strain values from specimens of block 4 were much lower than the specimens from the remaining block. For the sake of brevity and clarity, the sources of these variations are discussed in detail in the latter parts of this discussion. Also, by grouping the measurements by the source material, it can be noticed that the spread in mechanical properties of material form individual blocks of AM material is similar to that of cold rolled annealed material.

The values of maximum strain were noticed to vary significantly corresponding to the varying gage lengths for both cold rolled annealed and AM materials. It is well established that varying gage length produces different measurements of ductility. Also, geometrically similar specimens are expected to yield similar measurements. However, the similarity only minimizes the difference but does not eliminate it. The maximum strain measured during tensile tests is comprised of the elastic deformation, elongation from uniform plastic deformation (volume constancy relation holds true) and localized deformation i.e. necking. The amount of elastic deformation is negligible in comparison to the plastic deformation. The strain from uniform plastic deformation would be similar for specimens of all gage lengths as it is dependent on the material properties and not the gage length. The elongation from necking is also expected to be the same for all gage lengths as, all the specimens have the same cross section (nominal 1mm x 1mm). However, as the gage length increases the contribution of elongation from necking to the maximum strain value decreases (necking elongation is divided by larger gage length values). This decrease is seen in the maximum strain values of both AM and cold rolled annealed materials. The total elongation after neglecting elastic deformation can be represented in relation to the gage length as written below

$$u_T = GL * e_u + \alpha$$

Where $u_T$ is the total elongation, GL is the gage length, $\alpha$ is the elongation from necking and $e_u$is the strain corresponding to uniform plastic deformation.

In order to decouple strain measurements and estimate the strain corresponding to uniform plastic deformation and localized deformation, a regression analysis was performed. The analysis was performed to establish the linear empirical relationship between the total elongation

and the nominal gage length of the specimens. The elongation values calculated from the maximum strain measurements were fit against the nominal gage lengths. The SAS software was used to perform these linear fits. The intercept of the linear fit would be an estimate of the contribution in elongation from localized deformation. The slope of the linear fit would be an estimate for the strain that corresponds to uniform plastic deformation. The estimated values of slope and intercept from the linear fits for both cold rolled annealed and AM materials are listed in Table 2. The higher values of slope and intercept of the cold rolled annealed material imply that cold rolled annealed material is better than AM material in terms of ductility. The slope value for cold rolled annealed material implies that the cold rolled annealed material can undergo larger uniform plastic deformation than AM material. The higher value of intercept suggests that cold rolled annealed material necks larger than the AM material. The higher standard error values for slope and intercept estimates of AM material implies higher variability in ductility and lower consistency in performance when compared to the cold rolled annealed material (as seen from Figures 6 and 7). This also concludes the cold rolled annealed material is better than AM material in terms of toughness (area under the stress strain curves as seen from Figures 6 and 7).

Table 2. Slope and intercept values of linear fit between total elongation and nominal gage length

| | Cold rolled annealed material | | AM material | |
|---|---|---|---|---|
| Variable | Parameter Estimate | Standard Error | Parameter Estimate | Standard Error |
| $\alpha$ | 1.216mm | 0.023 | 0.545mm | 0.129 |
| $e_u$ | 0.688 | 0.005 | 0.467 | 0.029 |

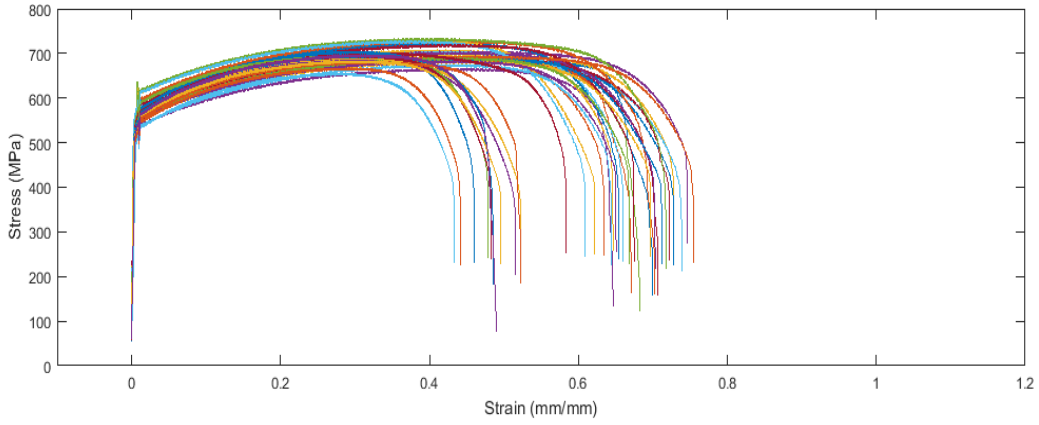


Figure 6. Engineering stress strain curves for mini tensile specimens of 3mm gage length made from AM 304L stainless steel

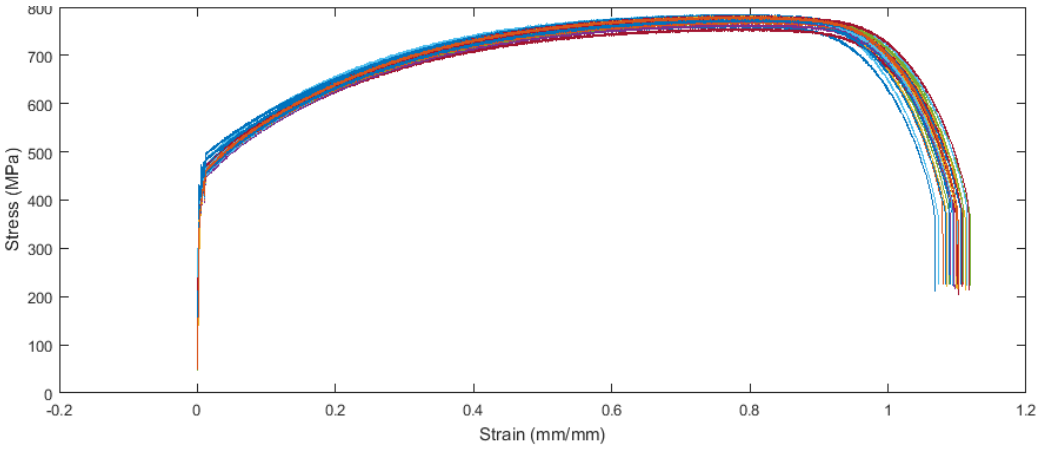

Figure 7. Engineering stress strain curves for mini tensile specimens of 3mm gage length made from cold rolled annealed 304L stainless steel

Empirical cumulative probability distributions of yield strength, ultimate strength, and maximum strain were plotted using two-parameter and three-parameter Weibull distributions. The American society of testing and materials standards C1683 and C1239 outline the basis and methodology for performing statistical analysis on material properties of advanced ceramic materials. However, the Weibull distribution has also been used to model the stochastic performance of metals (S. Karnati et al. 2016; J.W. Newkirk, T. Amine, and J. Koth 2016; J.W. Newkirk and J. Wang 2014; Salzbrenner et al. 2017). The equations of two-parameter and three-parameter Weibull distributions are as follows,

$$P(x) = \left(\frac{m}{\beta}\right)\left(\frac{x}{\beta}\right)^{m-1} exp\left[-\left(\frac{x}{\beta}\right)^{m}\right], x > 0$$

$$P(x) = \left(\frac{m}{\beta}\right)\left(\frac{x-\theta}{\beta}\right)^{m-1} exp\left[-\left(\frac{x-\theta}{\beta}\right)^{m}\right], x > 0, \theta > 0$$

Where P is the probability of event the occurring, x is the random variable, m is the Weibull modulus or shape parameter, β is the scale or characteristic value and θ is the threshold value. Weibull modulus or the shape parameter describes the breadth of the distribution. Higher the value of the Weibull modulus, lower is the spread of the distribution. The three parameter Weibull distribution can be used to model data where the possibility of failure under a certain value of the random variable has zero probability. The threshold value is an estimate of the value under which the probability of failure occurring is equal to zero.

The yield strength values from both materials were found to be a better fit for three-parameter Weibull distributions. The ultimate strength and maximum strain values were fit using a two-parameter Weibull distribution. The type of fit was chosen basing on the Akaike and

Bayesian information criterion provided by JMP software. The Weibull fits were performed using JMP software by following the maximum likelihood approach. The plots of these fits were made using Minitab software. The Weibull distribution plots for yield strength and 95% confidence intervals for the threshold, Weibull modulus, and characteristic strength were as shown in Figures 8, 9 and 10. The 95% confidence intervals of the distribution parameters for ultimate strength and maximum strain measurements and corresponding Weibull distribution plots are shown in Figures 11, 12, 13, 14 and 15.

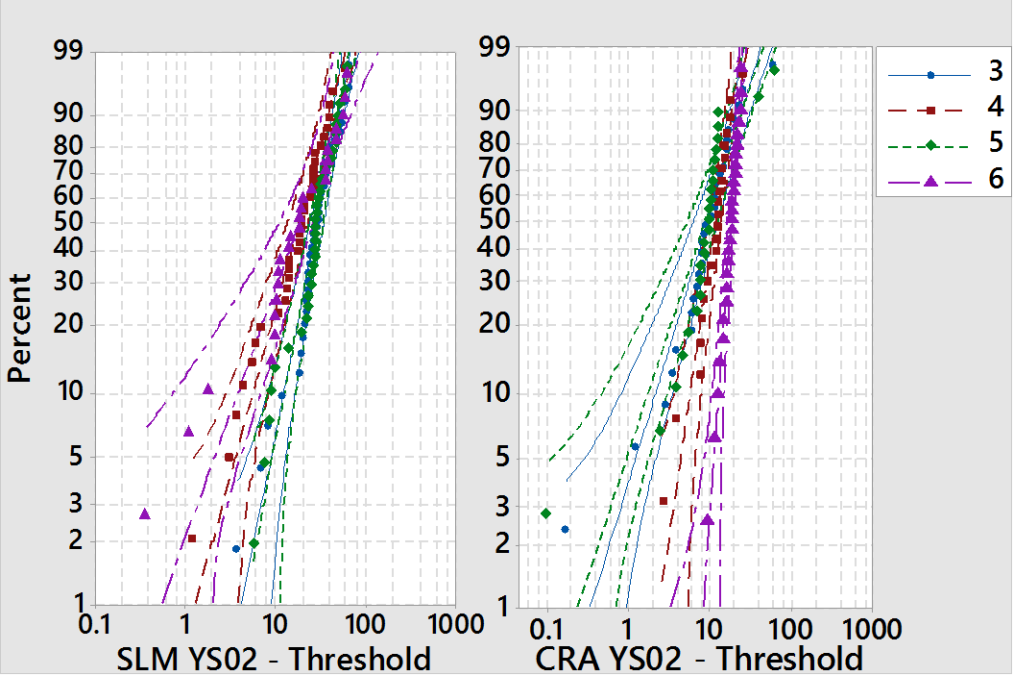


Figure 8. Cumulative three-parameter Weibull fits of the yield strength data obtained from specimens of SLM and cold rolled annealed (CRA) materials. The gage lengths are 3 (blue), 4 (red), 5 (green) and 6 (purple)

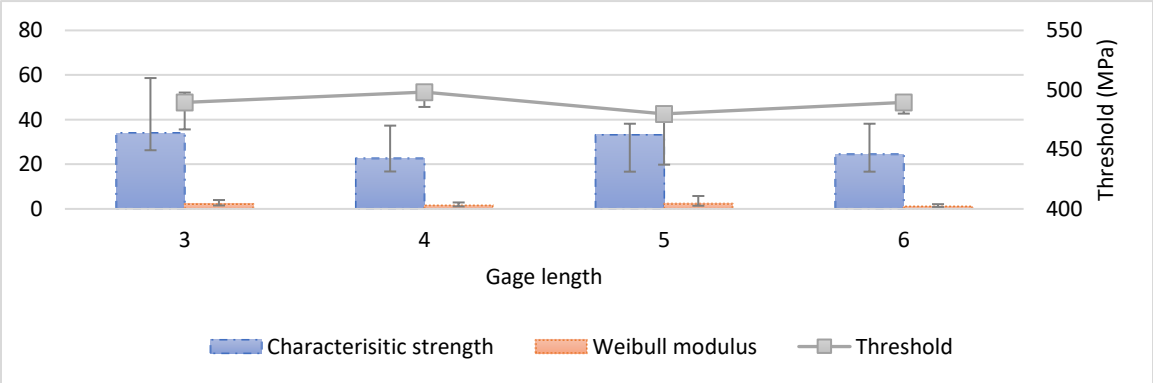


Figure 9. 95% confidence intervals for the three parameters fits of AM/SLM material shown in Figure 8

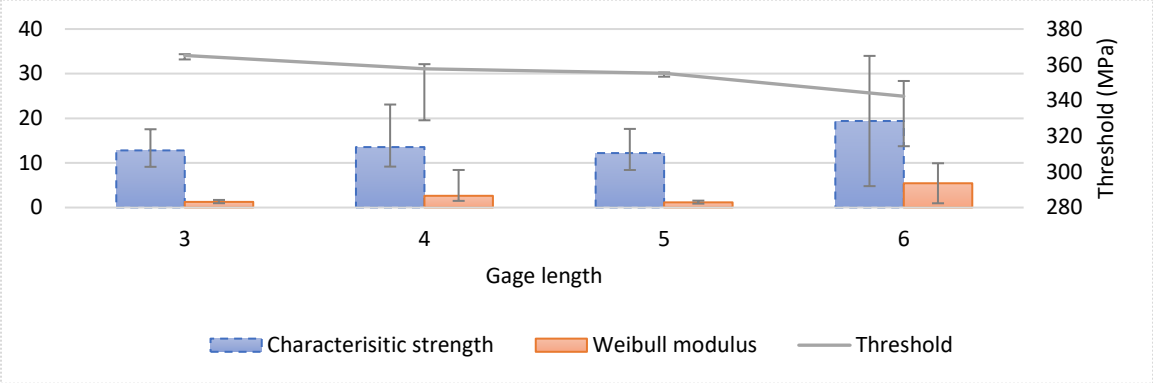


Figure 10. 95% confidence intervals for the three parameters fits of cold rolled annealed material shown in Figure 8

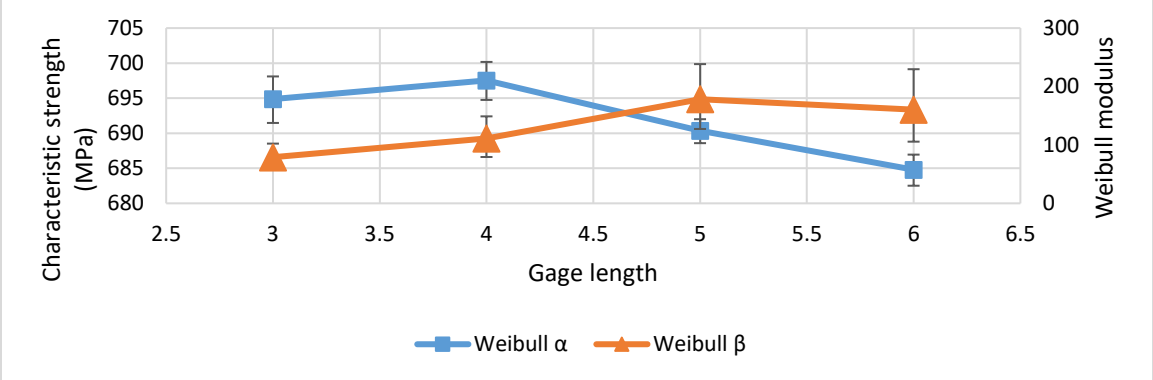


Figure 11. 95% confidence intervals of two-parameter Weibull fit (see Figure 15) on ultimate strength data of SLM/AM material. Weibull α is the characteristic strength and Weibull β is the Weibull modulus

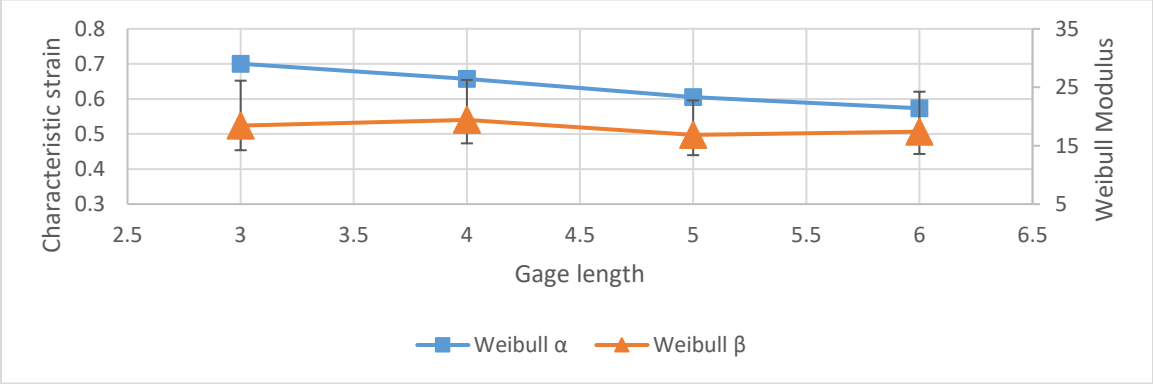


Figure 12. 95% confidence intervals of two-parameter Weibull fit (see Figure 15) on maximum strain data of SLM/AM material. Weibull α is the characteristic strain and Weibull β is the Weibull modulus

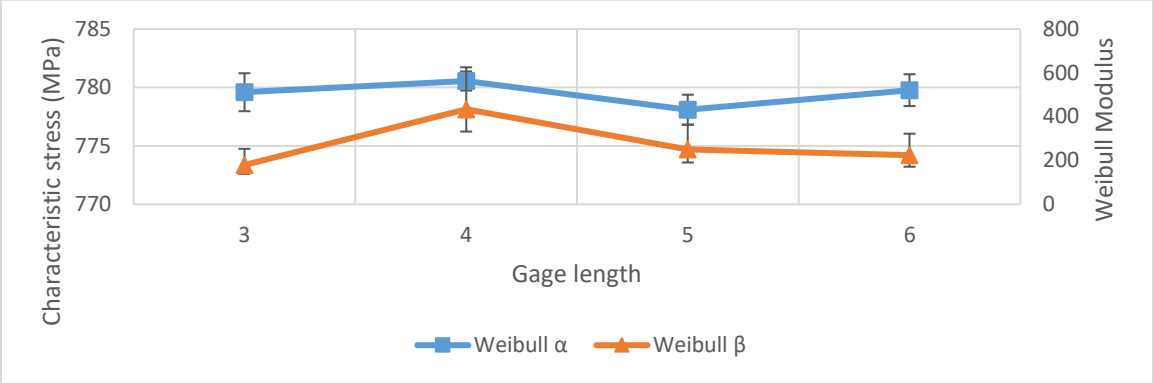


Figure 13. 95% confidence intervals of two-parameter Weibull fit (see Figure 15) on ultimate strength data of cold rolled annealed material. Weibull α is the characteristic strength and Weibull β is the Weibull modulus

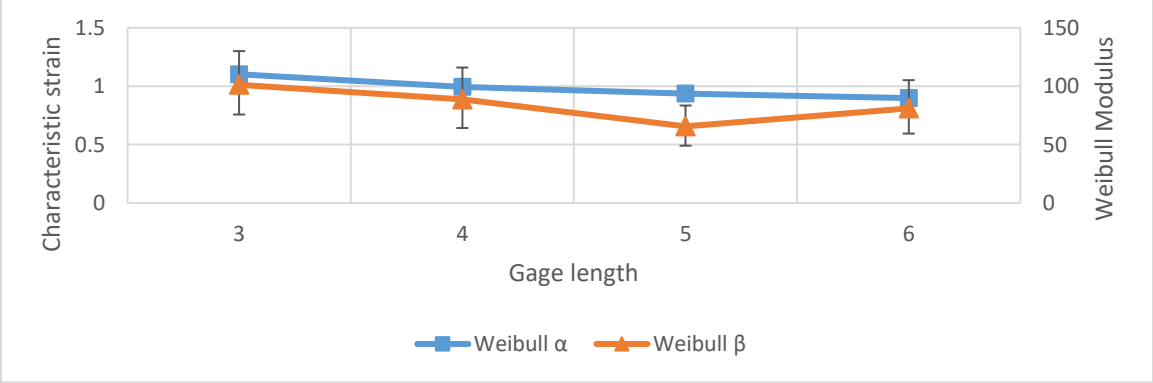


Figure 14. 95% confidence intervals of two-parameter Weibull fit (see Figure 15) on maximum strain data of cold rolled annealed material. Weibull α is the characteristic strain and Weibull β is the Weibull modulus

The Figures 10-17 give a good picture of the tensile stochastic performance of the cold rolled annealed and powder bed AM materials. The previously identified decreasing trends in yield strength measurements for cold rolled annealed material and maximum strain measurements of both cold rolled annealed and AM materials can also be seen from these Weibull statistics. The decreasing trend in threshold values of yield strength for cold rolled annealed materials indicates the drop in measured values of yield strength with increasing gage length. The Weibull moduli of both AM and SLM materials are comparable and do not vary significantly with increasing gage lengths.

The characteristic strain values for both cold rolled annealed and AM material indicate a drop in the measured values with increasing gage length. The Weibull modulus of strain for the

cold rolled annealed material is substantially higher than that of AM material. This is indicative of the better performance of the cold rolled annealed material and the large variability in ductility of the AM material. The same conclusions apply to the ultimate strength data as well. For some of the cases, the 95% confidence intervals were very wide and have significant overlap. A larger sample size can help decrease the error and provide better estimates to help resolve these overlaps. At this point, no change is observed in Weibull statistics with increasing gage length.

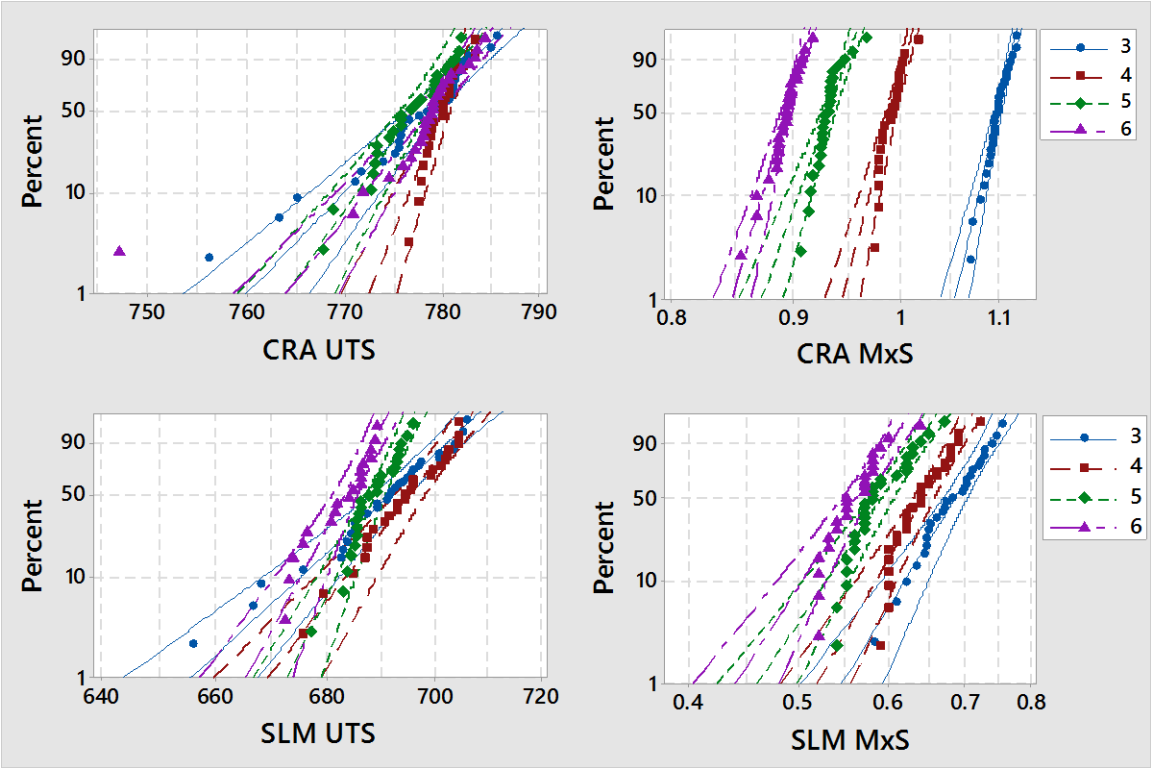


Figure 15. Two-parameter Weibull distributions of ultimate strength (UTS) and maximum strain (MxS) for cold rolled annealed and SLM/AM material. The different gage lengths are 3 (blue), 4 (red), 5 (green) and 6 (purple)

The lower performance of the AM material in terms of ultimate strength and ductility was investigated by analyzing the images of all the fracture surfaces gathered from the broken specimens of 3mm gage length. The specimens yielding high values of yield strength and ultimate strength, in general, had minimal porosity. The total porosity was made up of gas (spherical) and lack of fusion (irregular and along the direction of build) porosities. Specimens with lower strengths were observed to contain pores on the fracture surface.

The fracture surfaces of specimens yielding highest and lowest values of strength and ductility are shown in Figure 16. The specimen that yielded the highest strength values was

observed to have minimal porosity (Figure 16a). However, the specimen that yielded the highest strain (Figure 16b) was observed to have spherical pores on the fracture surface. The authors theorize this discrepancy can be attributed to the strain component stemming from localized deformation i.e. necking. The specimen in Figure 16a has a larger cross sectional area in comparison to the specimen in Figure 16b. This is indicative of necking to a larger extent in specimen shown in Figure 16b. The difference in elongation from necking produces a higher strain measurement and is therefore not a true representation of the specimen ductility.

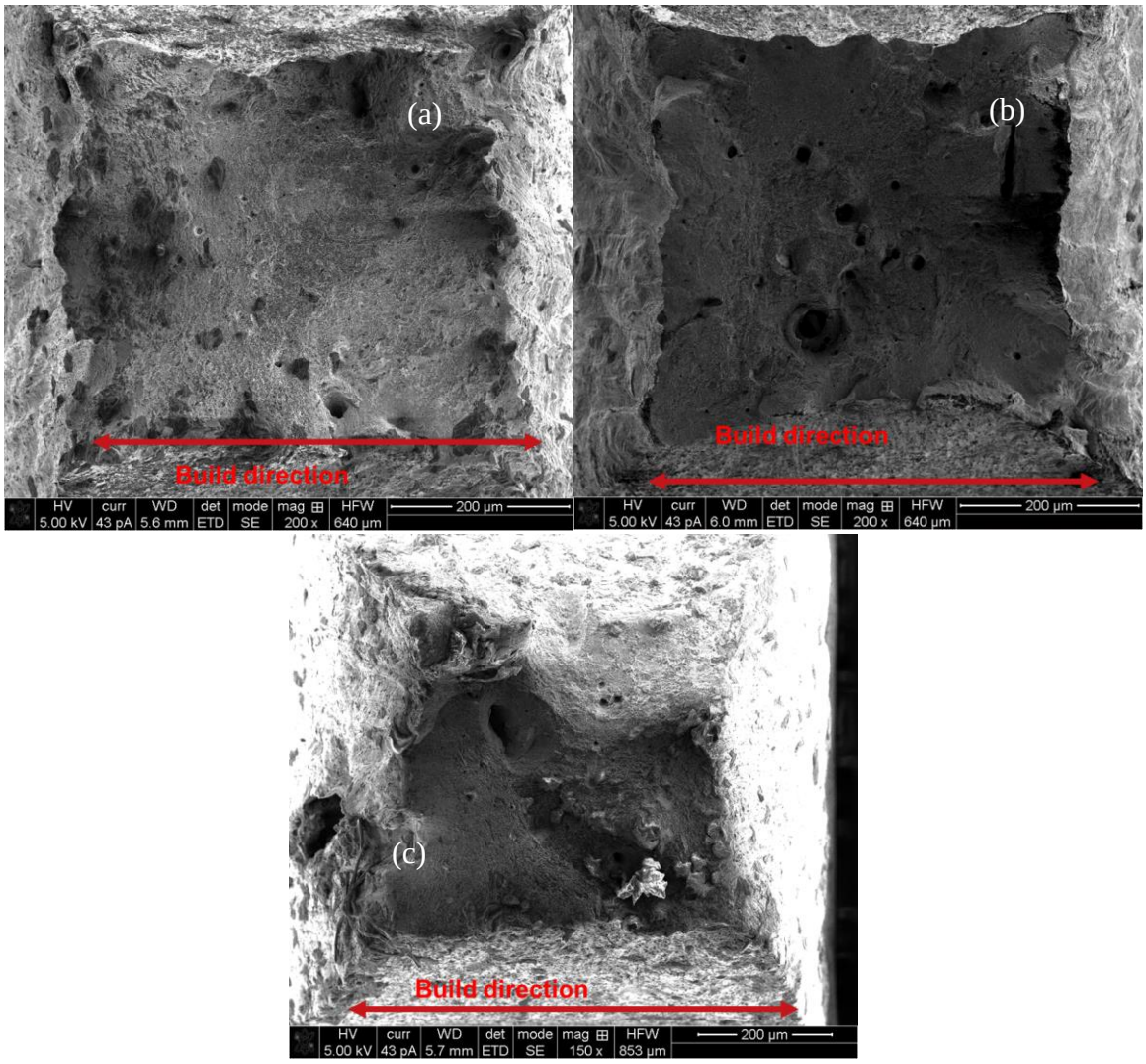


Figure 16. Secondary electron images of the fracture surfaces of (a) a specimen from block 2 with highest measured values of yield and ultimate strength (b) a specimen from block 1 with highest measured value of maximum strain and (c) a specimen from block 4 with the lowest measured values of yield strength, ultimate strength and maximum strain

By this reasoning, the lower performance of strain in specimens from block 4 could possibly be attributed to the difference in necking elongation. However, this needs a more detailed study into the reasoning behind the early fracture of these specimens. The specimens that yielded the lowest values of strength and strain was observed to have a lack of fusion pores across the cross section of the specimen.

## Conclusions

The current effort involved the fabrication and testing of mini tensile specimens of different gage lengths from conventional and powder bed AM fabricated 304 SS. To assess the impact of gage length, the measured values of 0.2% offset yield strength, ultimate tensile strength and maximum strain were analyzed and the following conclusions were made

- Analysis of variance revealed a significant impact of gage length on the maximum strain measurements. With the increase in gage length, the maximum strain values were observed to decrease. This was attributed to the decreasing contribution of localized deformation to maximum strain values
- A regression analysis was performed to estimate the strain corresponding to uniform plastic deformation and localized deformation. The analysis revealed the cold rolled annealed material was more ductile and tougher than the powder bed AM material
- The yield strength of powder bed AM material was observed to be higher than the cold rolled annealed material. However, the ultimate strength and maximum strain values of AM material were lower than those of cold rolled annealed material
- The variability in powder bed AM material was observed to be higher than the cold rolled annealed material. The wide variability in AM material was identified to be associated with the differences in the source material used to fabricate the different mini tensile specimens
- Weibull statistics were also performed on these tensile property measurements. The estimates from the Weibull fits were in accordance with the conclusions from analysis of variance.
- The Weibull estimates for the yield strength of cold rolled annealed and AM material were comparable and has similar Weibull moduli. The estimated values of Weibull moduli for ultimate strength and maximum strain also corroborated the wide variance in performance of powder bed AM material
- Investigation of fracture surfaces revealed porosity was the cause for such wide variability
- Finally, the mini tensile specimens were able to produce repeatable and reliable measurements of the tensile properties of conventional and powder bed fabricated AM materials. These specimens were also able to capture the source to source variation in terms of strength and ductility

## Acknowledgments

This work has been funded by Honeywell Federal Manufacturing & Technologies under Contract No. DE-NA0002839 with the U.S. Department of Energy. The United States Government retains and the publisher, by accepting the article for publication, acknowledges that the United States Government retains a nonexclusive, paid up, irrevocable, world-wide license to publish or reproduce the published form of this manuscript, or allow others to do so, for the United States Government purposes.

Furthermore, the authors would like to acknowledge Kyle Stagner, Ian Wille, and Brian Bullock for their aid in this research.

## References

Blackwell, P.L. 2005. "The Mechanical and Microstructural Characteristics of Laser-Deposited IN718." *Journal of Materials Processing Technology* 170 (1): 240–46. doi:10.1016/j.jmatprotec.2005.05.005.

Dieter, George E. 1986. *Mechanical Metallurgy*. McGraw-Hill.

Gao, Wei, Yunbo Zhang, Devarajan Ramanujan, Karthik Ramani, Yong Chen, Christopher B. Williams, Charlie C.L. Wang, Yung C. Shin, Song Zhang, and Pablo D. Zavattieri. 2015. "The Status, Challenges, and Future of Additive Manufacturing in Engineering." *Computer-Aided Design* 69: 65–89. doi:10.1016/j.cad.2015.04.001.

J.W. Newkirk, and J. Wang. 2014. "Mechanical Testing Of PM Parts Using Sub-Size Specimens." *Advances in Powder Metallurgy & Particulate Materials* 11: 16–22.

J.W. Newkirk, T. Amine, and J. Koth. 2016. "Tensile Test Methodology for PM Components." In *PowderMet16*.

Kumar, Kundan, Arun Pooleery, K. Madhusoodanan, R.N. Singh, J.K. Chakravartty, B.K. Dutta, and R.K. Sinha. 2014. "Use of Miniature Tensile Specimen for Measurement of Mechanical Properties." *Procedia Engineering* 86: 899–909. doi:10.1016/j.proeng.2014.11.112.

Lord, J. D., B. Roebuck, R. Morrell, and T. Lube. 2010. "Aspects of Strain and Strength Measurement in Miniaturised Testing for Engineering Metals and Ceramics." *Materials Science and Technology* 26 (2). Taylor & Francis: 127–48. doi:10.1179/026708309X12584564052012.

"Metal Additive Manufacturing Processes." 2017. http://www.metal-am.com/introduction-to-metal-additive-manufacturing-and-3d-printing/metal-additive-manufacturing-processes/.

N. F. Panayotou, S. D. Artkin, R. J. Puigh, B. A. Chin. 1986. "Design and Use of Nonstandard Tensile Specimens for Irradiated Materials Testing." In *ASTM STP 888. W.R. Corwin Y G. E. Lucas, Eds., American Society for Testing and Materials, Philadelphia*, 201–19. 100 Barr Harbor Drive, PO Box C700, West Conshohocken, PA 19428-2959: ASTM International. doi:10.1520/STP33004S.

Olakanmi, E.O., R.F. Cochrane, and K.W. Dalgarno. 2015. “A Review on Selective Laser Sintering/melting (SLS/SLM) of Aluminium Alloy Powders: Processing, Microstructure, and Properties.” *Progress in Materials Science* 74: 401–77. doi:10.1016/j.pmatsci.2015.03.002.

Rao, Heng, Stephanie Giet, Kun Yang, Xinhua Wu, and Chris H.J. Davies. 2016. “The Influence of Processing Parameters on Aluminium Alloy A357 Manufactured by Selective Laser Melting.” *Materials & Design* 109: 334–46. doi:10.1016/j.matdes.2016.07.009.

Rosinski, S., A. Kumar, N. Cannon, and M. Hamilton. 1993. *Application of Subsize Specimens in Nuclear Plant Life Extension*. West Conshohocken, PA: ASTM International. doi:https://doi.org/10.1520/STP12744S.

S. Karnati, I. Axelsen, F. F. Liou, and J. W. Newkirk. 2016. “Investigation Of Tensile Properties Of Bulk and SLM Fabricated 304L Stainless Steel Using Various Gage Length Specimens.” In *Proceedings of the 27th Solid Freeform Fabrication Symposium*, 592–604. Austin.

Salzbrenner, Bradley C., Jeffrey M. Rodelas, Jonathan D. Madison, Bradley H. Jared, Laura P. Swiler, Yu Lin Shen, and Brad L. Boyce. 2017. “High-Throughput Stochastic Tensile Performance of Additively Manufactured Stainless Steel.” *Journal of Materials Processing Technology* 241 (241): 1–12. doi:10.1016/j.jmatprotec.2016.10.023.

Shamsaei, Nima, Aref Yadollahi, Linkan Bian, and Scott M. Thompson. 2015. “An Overview of Direct Laser Deposition for Additive Manufacturing; Part II: Mechanical Behavior, Process Parameter Optimization and Control.” *Additive Manufacturing* 8: 12–35. doi:10.1016/j.addma.2015.07.002.

Song, Bo, Xiao Zhao, Shuai Li, Changjun Han, Qingsong Wei, Shifeng Wen, Jie Liu, and Yusheng Shi. 2015. “Differences in Microstructure and Properties between Selective Laser Melting and Traditional Manufacturing for Fabrication of Metal Parts: A Review.” *Frontiers of Mechanical Engineering* 10 (2). Higher Education Press: 111–25. doi:10.1007/s11465-015-0341-2.

Yadollahi, Aref, Scott M. Thompson, Alaa Elwany, and Linkan Bian. 2017. “Effects of Building Orientation and Heat Treatment on Fatigue Behavior of Selective Laser Melted 17-4 PH Stainless Steel.” *International Journal of Fatigue* 94: 218–35. doi:10.1016/j.ijfatigue.2016.03.014.